AGU PUBLICATIONS

Water Resources Research

RESEARCH ARTICLE

10.1002/2016WR018607

Key Points:

- Terrestrial hydrological sensitivity is 3 times greater in wet regions than dry regions
- A greater detectability of hydrological changes in wet regions than dry regions
- Reduction in catchment efficiency parameter opposes the effects of increasing evaporative demand

Supporting Information:

- Supporting Information S1

Correspondence to:
S. Kumar,
Sanjiv.Kumar@noaa.gov

Citation:
Kumar, S., F. Zwiers, P. A. Dirmeyer, D. M. Lawrence, R. Shrestha, and A. T. Werner (2016), Terrestrial contribution to the heterogeneity in hydrological changes under global warming, *Water Resour. Res.*, *52*, 3127–3142, doi:10.1002/2016WR018607.

Received 12 JAN 2016
Accepted 23 MAR 2016
Accepted article online 28 MAR 2016
Published online 22 APR 2016

Terrestrial contribution to the heterogeneity in hydrological changes under global warming

Sanjiv Kumar[1,2], Francis Zwiers[1], Paul A. Dirmeyer[3], David M. Lawrence[4], Rajesh Shrestha[1], and Arelia T. Werner[1]

[1]Pacific Climate Impacts Consortium, University of Victoria, Victoria, British Columbia, Canada, [2]Now at NOAA/ESRL Physical Science Division, Boulder, Colorado, USA, [3]Center for Ocean-Land-Atmosphere Studies, George Mason University, Fairfax, Virginia, USA, [4]National Center for Atmospheric Research, Boulder, Colorado, USA

Abstract This study investigates a physical basis for heterogeneity in hydrological changes, which suggests a greater detectability in wet than dry regions. Wet regions are those where atmospheric demand is less than precipitation (energy limited), and dry regions are those where atmospheric demand is greater than precipitation (water limited). Long-term streamflow trends in western North America and an analysis of Coupled Model Intercomparison Project Phase 5 (CMIP5) climate models at global scales show geographically heterogeneous detectability of hydrological changes. We apply the Budyko framework and state-of-the-art climate model data from CMIP5 to quantify the sensitivity and detectability of terrestrial hydrological changes. The Budyko framework quantifies the partitioning of precipitation into evapotranspiration and runoff components. We find that the terrestrial hydrological sensitivity is 3 times greater in regions where the hydrological cycle is energy limited rather than water limited. This additional source (the terrestrial part) contributes to 30–40% greater detectability in energy-limited regions. We also quantified the contribution of changes in the catchment efficiency parameter that oppose the effects of increasing evaporative demand in global warming scenarios. Incorporating changes to the catchment efficiency parameter in the Budyko framework reduces dry biases in global runoff change projections by 88% in the 21st century.

1. Introduction

Reliable water availability (streamflow) projections are important for a number of economic sectors including agriculture, water supply, and energy. However, there exist large uncertainties in hydrological projections that arise from multiple sources including global climate models, emission scenarios, model parametrizations, downscaling methodology, hydrologic modeling, and internal variability in the climate system [*Haddeland et al*., 2011; *Hagemann et al*., 2011; *Deser et al*., 2012; *Chen et al*., 2013; *Vano et al*., 2013]. Observed hydrological changes show significant spatial heterogeneity with instances of increasing, decreasing, and no significant streamflow trends found in the historical period [*Milly et al*., 2005; *Dai et al*., 2009; *Stahl et al*., 2010; *Sagarika et al*., 2014]. The observed changes are also confounded by the uncertainties in data, methodology, and metrics of hydrological changes [*Kumar et al*., 2009; *Sheffield et al*., 2012; *Allan*, 2014; *Greve et al*., 2014; *Trenberth et al*., 2014]. While prior studies have found some evidence of human influence on precipitation changes, the detection of global streamflow changes is not robust [*Zhang et al*., 2007; *Dai et al*., 2009; *Alkama et al*., 2013; *Jimenez Cisneros et al*., 2014; *Wan et al*., 2014]. *Greve et al*. [2014] and *Greve and Seneviratne* [2015] have found significant uncertainties in hydrological changes over land that can be due to internal climate variability, and water limitations to evaporation over land [*Kumar et al*., 2015].

To navigate this cloud of uncertainties, it is important to understand the underlying physical processes that, when isolated, are robust indicators of future hydrological changes. One such feature is greater detectability of hydrological changes in wet regions than dry regions (Figures 1 and 2; discussed later) referred to as heterogeneity in hydrological changes, hereafter. Wet regions are defined as those where atmospheric demand is less than precipitation and dry regions are those where atmospheric demand is greater than precipitation. Wet and dry regions can be defined on the global or regional scales. Different climate extremes have been observed in wet and dry regions recently, e.g., 2015 South Carolina Flood (a wet region), and 2012–2015 California drought (a dry region). An improved understanding of the physical processes leading to

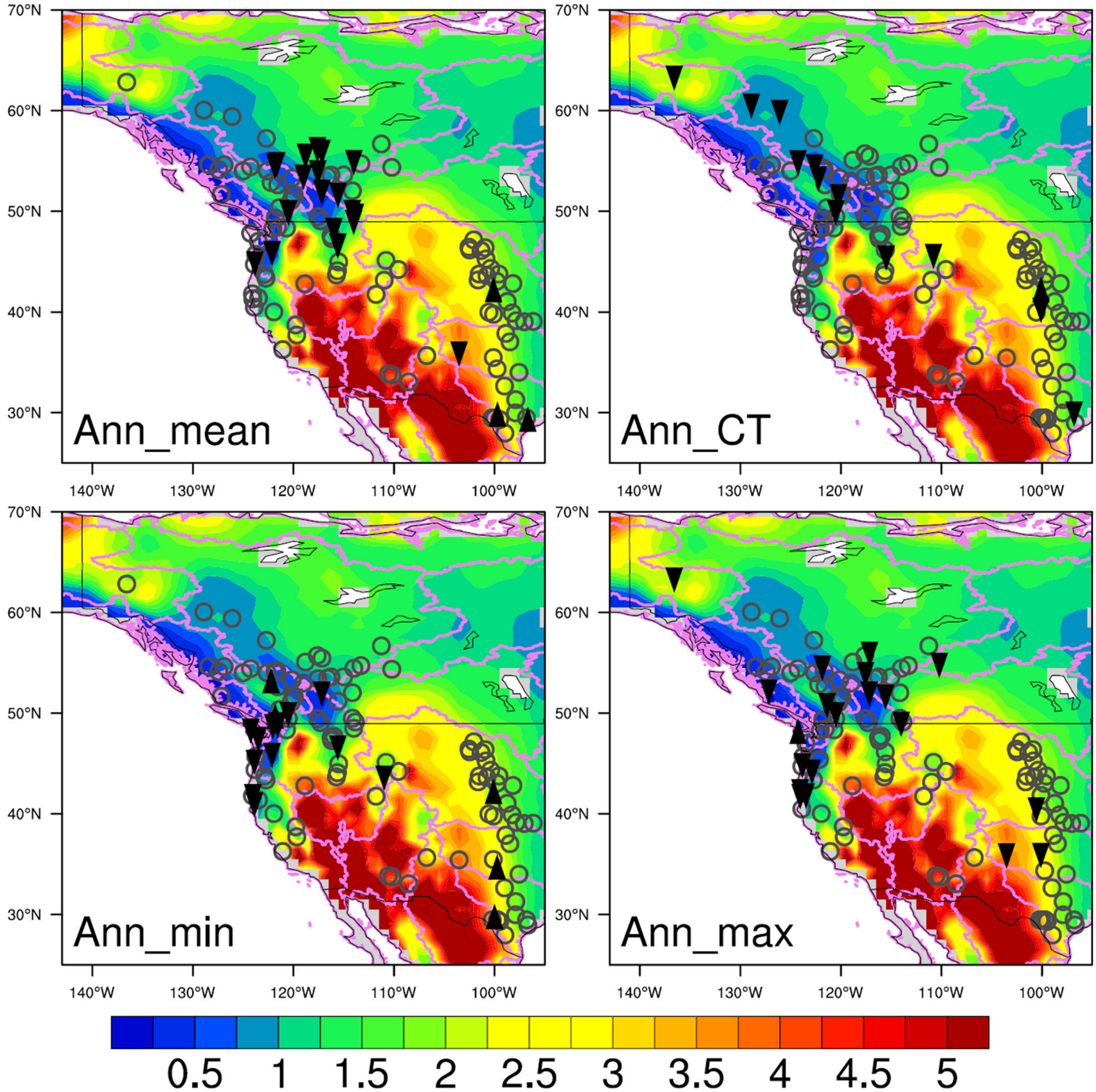

Figure 1. Long-term trends (1951–2010) in streamflow observations in 115 watersheds across western North America. Increasing trends that are statistically significant at the 5% level are shown by up arrows, and decreasing trends by down arrows. Insignificant trends are shown by gray circles. Trends are calculated using a nonparametric method and considering long-term persistence in the time series (see section 2). The four hydrologic change indicators shown here are: (a) Ann_mean: annual average flow, (b) Ann_CT: timing for half of the annual flow or center of timing, (c) Ann_min: annual minimum flow, and (d) Ann_max: annual maximum flow. Color shading shows estimated DI from global observations.

heterogeneity in hydrological changes can be helpful in regional-scale detection and attribution studies [e.g., *Herring et al.*, 2014; *Seager et al.*, 2015].

While prior studies have investigated contributions of the atmospheric branch of the hydrological cycle, e.g., increased water vapor concentration and circulation changes [*Chou and Neelin*, 2004; *Held and Soden*, 2006; *Santer et al.*, 2007; *Seager et al.*, 2010; *Chadwick et al.*, 2012], such contributions from the terrestrial

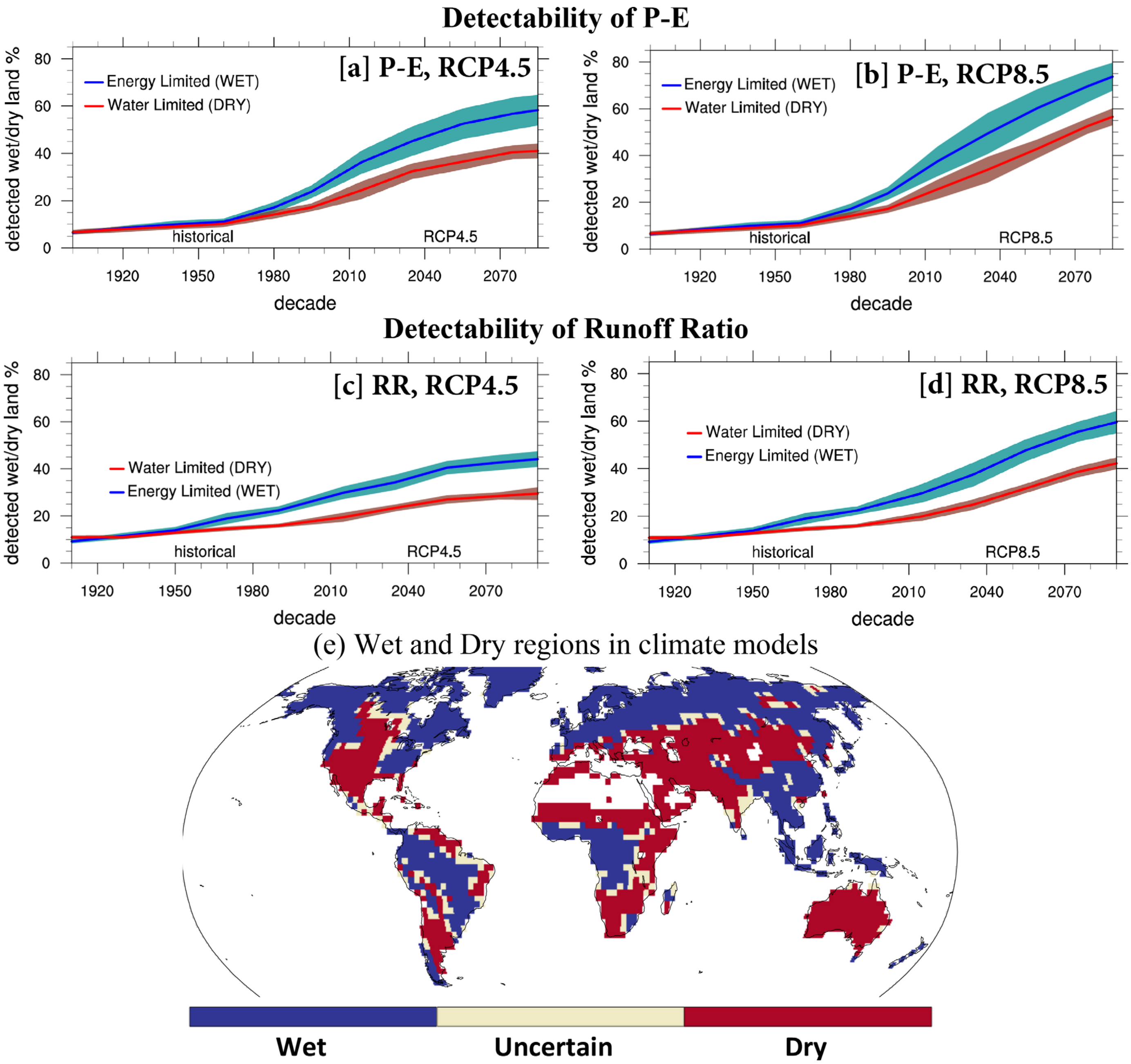

Figure 2. Time series of detectability of changes in P-E and runoff ratio (RR) under global warming scenarios: (a and c) Historical + RCP4.5 and (b and d) Historical + RCP8.5, all relative to preindustrial climate simulations. Multimodel mean computed from four CMIP5 climate models (CanESM2, CCSM4, CNRM-CM5, and MPI-ESM-MR; see text). Shading represents 95% confidence interval uncertainty range of multimodel mean. Wet and dry regions are defined based on majority rule (≥three out of four models). Uncertain areas represent equal division between four models, i.e., two models dry and two models wet. Threshold DI for wet and dry regions is selected such that all land areas (except Antarctica and Sahara deserts) are equally divided between wet and dry regions, i.e., 50% each in individual models' preindustrial climate.

branch of the hydrological cycle, namely the partitioning of precipitation into evapotranspiration and runoff, have not been investigated to the same degree, e.g., in terms of differences between wet and dry regions. The primary goal of this study is to elucidate the roles of the terrestrial branch of the hydrological cycle. The terrestrial branch can contribute to the heterogeneity in hydrological changes through: (1) greater soil water storage capacity in dry regions than wet regions (discussed later) and (2) increased plant water use efficiency under elevated atmospheric CO_2 concentrations [*Betts et al.*, 2013; Cao et al., 2010]. We also investigate the major source of uncertainty that may strengthen or weaken the heterogeneity in hydrological changes (discussed later).

The Budyko framework is a heuristic approach to conceptually partition precipitation into evapotranspiration and streamflow using just a few model parameters [*Budyko*, 1958]. The Budyko framework has been tested, validated, and applied in numerous observational and modeling-based studies, and remains an active research area [*Milly*, 1994; *Koster and Suarez*, 1999; *Zhang et al*., 2001, 2004, 2008; *Berghuijs et al*., 2014; *Greve et al*., 2014, 2015]. *Koster* [2014] found that the Budyko framework performs better than several land surface models in describing the relationship between evapotranspiration and runoff efficiencies. *Roderick et al*. [2014] found that climate model projections of precipitation and evapotranspiration closely follow the Budyko framework. However, they did not consider the sensitivity to changes in model parameters, which is an important aspect (shown later). We apply the Budyko framework in combination with other data and methods to study sensitivity and detectability of hydrological changes.

Zhang et al. [2004] presented a physical basis for the Budyko framework that is based on the complementary relationship between water and energy. In general, the Budyko framework is a demand to supply framework that can be used to predict water availability at annual and subseasonal time scales [*Zhang et al*., 2008]. *Li et al*. [2013] found a significant positive relationship between the Budyko model parameter and vegetation coverage for large catchments around the world. A secondary goal of this study is to understand future hydrological changes predicted by state-of-the-art coupled climate and earth system models [*Taylor et al*., 2011; *Flato et al*., 2013] in the context of the Budyko framework and identify its major sources of uncertainty for using the Budyko framework in future water prediction. The state-of-the-art coupled climate and earth system models represent our best approximation of future water availability because they are backed with our most up-to-date representation of the physical processes, e.g., coevolution of carbon-water-energy cycles, prognostic vegetation phenology scheme, and land use change in Community Land Model [*Oleson et al*., 2010; *Lawrence et al*., 2011].

2. Data and Methods

Streamflow Data. We employed streamflow observations for 115 natural or near-natural watersheds in western North America (supporting information Table S1). Long-term trends (>50 years) are calculated using the nonparametric Theil-Sen method and trend significance is determined using the Mann-Kendall test considering long-term persistence in the time series as described in *Kumar et al*. [2009]. High-resolution (4 km) PRISM climate data [*Daly et al*., 2008] are employed in the Budyko modeling (described later) at the watershed scale.

CMIP5 Data. We extend our analysis globally and to future projections using climate model output from the CMIP5 archive [*Taylor et al*., 2011]. We use projections based on Representative Concentration Pathways RCP4.5—a medium emissions scenario with radiative forcing in year 2100 of 4.5 W m^{-2} and RCP8.5—a high emission scenario with a radiative forcing of 8.5 W m^{-2}. All available ensembles are employed; thus, a total of 88 historical climate simulations, 54 RCP8.5 and 15 RCP4.5 climate projections, and four 1000 year preindustrial climate simulations from 24 climate models are analyzed (supporting information Table S2). Our selection of CMIP5 models was limited by the availability of required variables for calculating potential evapotranspiration. To avoid biases caused by having more ensemble members from one climate model than another, we used a multimodel ensemble (MME) weighted average approach; thus, ensuring a "one model one vote" policy [Jones et al., 1969]. Climate model outputs were interpolated to a common 2.5° × 2.5° (72 × 144) resolution using an area average preserving method (http://www.ncl.ucar.edu/Document/Functions/Contributed/area_conserve_remap_Wrap.shtml).

Three global observational data sets were employed for CMIP5 model evaluation: (1) Climate Research Unit Time Series 3.10 (CRU TS3.1) [*Harris et al*., 2014], (2) Princeton Hydrology Data [*Sheffield et al*., 2012], and (3) CRU National Center for Environmental Predications Community Land Model offline forcing data (CRU-NCEP, ftp://nacp.ornl.gov/synthesis/2009/frescati/temp/land_use_change/original/readme.htm).

Potential evapotranspiration is calculated using the Penman-Monteith method employing the Food and Agricultural Organization grass reference evapotranspiration equation [*Allen et al*., 1994; *Harris et al*., 2014] and the following CMIP5 monthly variables were employed: near-surface air temperature, evaporation, surface upward sensible heat flux, near-surface relative humidity, eastward near-surface wind, and northward near-surface wind.

Table 1. Heterogeneous Detectability of Hydrological Changes[a]

Metric/Simulations	Energy Limited (Wet)	Water Limited (Dry)	Wet − dry%[b]
a. Detectability of Observed Hydrological Changes in Western North America (Unit: % of Stations Showing Significant Trends), cf. Figure 1			
Long-term trends in Annual Mean flow	25	14	56
Long-term trends in center of timing	14	9	43
Long-term trends in Annual Minimum flow	20	9	75
Long-term trends in Annual Maximum flow	22	13	51
b. Detectability of P-E Changes in Perfect Model Framework, cf. Figure 2a (Unit: % Areas Showing Significant Changes)			
Historical (1981–2000)	24 ± 3	17 ± 2	32
RCP4.5 (2081–2100)	58 ± 6	41 ± 3	35
RCP8.5 (2081–2100)	74 ± 6	57 ± 4	26
c. Detectability of RR Changes in Perfect Model Framework, cf. Figure 2b (Unit: % Areas Showing Significant Changes)			
Historical (1981–2000)	22 ± 2	16 ± 1	34
RCP4.5 (2081–2100)	44 ± 3	30 ± 3	40
RCP8.5 (2081–2100)	60 ± 5	42 ± 2	34

[a]Error bars show ±2 standard error estimate of mean detectability from four climate models.
[b]Wet − dry% = (wet − dry) ×100/[(wet + dry)/2].

The Budyko Framework and Terrestrial Hydrological Sensitivity. The water balance equation $(\Delta S = P - ET - R)$ can be combined with a formulation of the Budyko curve to obtain an analytical expression for runoff ratio (RR) [*Zhang et al*., 2008].

$$RR = -DI + \left[1 + DI^{w}\right]^{1/w} \tag{1}$$

where $RR = R/P$ is the runoff ratio, $DI = PET/P$ is a dryness index, and *PET*, *ET*, *P*, and *R* are potential evapotranspiration, actual evapotranspiration, precipitation, and total runoff, respectively. Over a climatological mean period, e.g., 20 year average, the change in storage is negligible $(\Delta S = 0)$. Parameter *w*, which depends on catchment characteristics such as topography, soil, vegetation, climate, and other environmental variables such as atmospheric CO_2 concentration, and land use change (discussed later) [also see *Roderick and Farquhar*, 2011] range from 1 to infinity [*Milly*, 1994; *Zhang et al*., 2008] and represent the efficiency of the catchment in converting precipitation into evapotranspiration. Higher *w* implies a higher *ET/P* ratio and thus a reduced runoff ratio, *R/P*. We employed a nonlinear optimization to estimate *w* using *RR* and *DI* data from observations or CMIP5 models and equation (1) (supporting information section S1).

The sensitivity of hydrological changes to global warming as measured by the changes in dryness index is given by,

$$\frac{dRR}{dDI} = \frac{\partial RR}{\partial DI} + \frac{\partial RR}{\partial w}\frac{dw}{dDI} \tag{2a}$$

where

$$\frac{\partial RR}{\partial DI} = -1 + \left[1 + DI^{w}\right]^{\left(\frac{1}{w}-1\right)} \cdot DI^{w-1} \tag{2b}$$

$$\frac{\partial RR}{\partial w} = \left[1 + DI^{w}\right]^{\frac{1}{w}} \cdot \left[\frac{DI^{w} \cdot \ln(DI)}{(DI^{w}+1) \cdot w} - \frac{\ln(DI^{w}+1)}{w^{2}}\right] \tag{2c}$$

This equation represents primarily the terrestrial contribution to the hydrological sensitivity because *RR*, to the first order, offsets the effect of precipitation changes, that is, to changes in the atmospheric branch of the hydrological cycle. The sensitivity of the catchment efficiency parameter $\left(\frac{dw}{dDI}\right)$ is estimated by fitting a second-degree polynomial to time series of estimated *ln*(*w*) and *DI* values using CMIP5 data for historical, and RCP8.5 climate simulations,

$$\ln(w) = CF_1 \cdot CF_2 \cdot \left[\beta_0 + \beta_1 \cdot DI + \beta_2 \cdot DI^{2}\right] \tag{3}$$

and then differentiating equation (3) with respect to *DI*. Here CF_1 represents the effects of vegetation changes, mainly due to conversion from natural vegetation to crop/grass land [*Zhang et al*., 2001], and CF_2 represents the effect of increased CO_2 concentrations on the plant transpiration in terms of increased water use efficiency and thereby a decrease in the catchment efficiency parameter [*Betts et al*., 2007; *Cao et al*., 2010]. CF_1 and CF_2 values are obtained from the literature and linearly interpolated to CMIP5 land use changes and atmospheric CO_2 concentration changes. Least squares estimates of polynomial coefficients β_1, β_2, and β_3 and their 95% confidence intervals are employed (see supporting information section S1 for details).

3. Results

3.1. Observational and Model-Based Evidence of Heterogeneity in Detection of Hydrological Changes

Figure 1 shows long-term trends (1951–2010) in annual average streamflow, center of timing for the annual flow, annual minimum flow, and annual maximum flow for 115 streamflow gauging stations in western North America along with an observational *DI* estimate. Figure 1 and Table 1 suggest that hydrological changes have been detected more frequently in energy-limited (wet) regions such as western Canada and the Pacific Northwest than in water-limited (dry) regions such as the western United States. For example, 25% of stations show significant trends in annual mean flow in energy-limited regions compared to only 14% in water-limited regions.

Figure 2 shows time series of detectability of P-ET and *RR* in historical and future climate simulations using perfect model analysis method described in *Kumar et al*. [2015]. We compared model simulated changes against internal climate variability that is determined from long (~1000 years) preindustrial climate simulations in four climate models [see *Kumar et al*., 2015 for details]. Globally, wet regions show 35% higher detectability in P-ET changes and 40% higher detectability in *RR* changes by the end of 21st century under the medium emission scenario (RCP4.5) than dry regions. Based on this evidence (Figures 1 and 2 and Table 1), we conclude that a greater detectability of hydrological change in wet regions than dry regions is an emerging feature of future hydrological change. Next, we investigate a physical basis for the heterogeneity in hydrological changes.

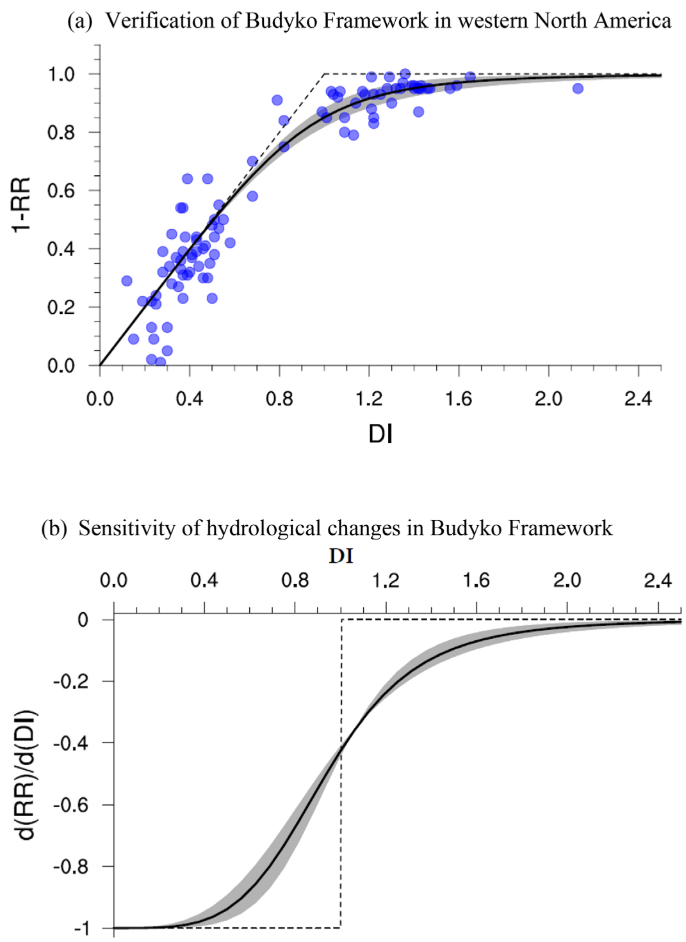

Figure 3. (a) Verification of the Budyko framework using 95 watersheds in western North America. High-resolution PRISM climate data were used to calculate *PET* using the Thornthwaite method because of limitations of data availability (e.g., relative humidity and wind are not available). Shaded regions show 95% confidence intervals based on nonlinear optimization of the *w*. Dashed lines show two limits: energy (sloped line) and water limits (horizontal line). (b) Theoretical sensitivity of hydrological changes in the Budyko framework (see text).

3.2. An Observational Context of Budyko-Based Terrestrial Hydrological Sensitivity

Figure 3a shows a validation of the Budyko curve (equation (1)) using a subset of 95 watersheds in western North America. Quality controlled high-resolution precipitation data are not available for the remaining 20 watersheds; hence they are not included (see supporting information section S2). The Budyko curve describes the climatological mean water availability (RR) with reasonable accuracy; the coefficient of determination (R^2) and the model efficiency coefficient are both 0.91 for the optimized $w = 5.0$. Some of

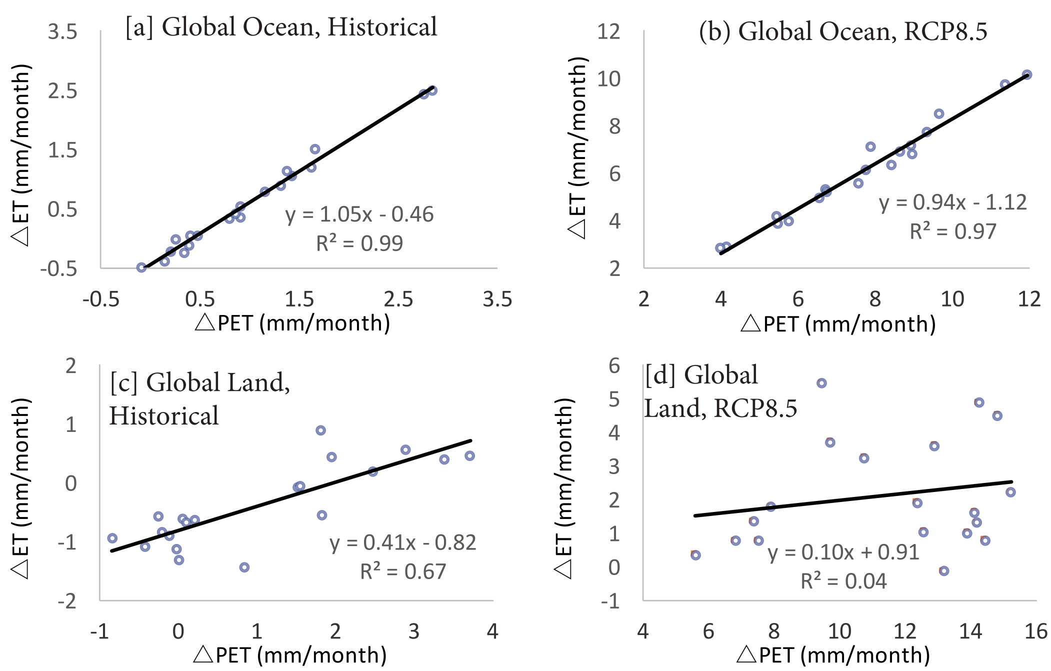

Figure 4. Evaluation of *PET* estimates in 20 CMIP5 climate models. *PET* is estimated using Penman-Monteith method (section 2) and *ET* is climate model outputs. (top row) Global ocean and (bottom row) global land, both 60°S–80°N. △ historical: (1981–2000) to (1881–1900); △ RCP8.5: (2081–2100) to (2006–2025).

the uncertainty in the Budyko framework in energy-limited regions (DI $<$ 1.0) can be due to underestimation in precipitation data that may be related to undercatch of precipitation measurements at high latitudes, e.g., British Columbia, and/or errors introduced with interpolation [*Groisman and Legates*, 1994; *Mekis and Vincent*, 2011] (supporting information section S2). We also found that equation (1) provides comparable estimates of *RR* in snow-dominated regions than using more sophisticated equations suggested by *Zhang et al*. [2015] (supporting information section S2).

Figure 3b shows the sensitivity of hydrological changes using only the first term in equation (2a), i.e., assuming change in the catchment efficiency parameter is negligible, an assumption that is relaxed later in the paper. It is evident that the estimated hydrological sensitivity is considerably larger in energy-limited regions than in water-limited regions. Verification of the estimate of hydrologic sensitivity based on the Budyko framework would require long-term century-scale observations that are unfortunately not available. We therefor analyze the CMIP5 simulations at global scales because wet-dry regions exist globally, and relatively coarse resolution CMIP5 data provide a meaningful result at global scales. However, before we discuss CMIP5 results, we address uncertainty in the *PET* estimate in view of recent literature [e.g., *Roderick et al*., 2015].

3.3. Addressing Uncertainty in Estimating *PET*

In this study, *PET* is measure of atmospheric demand, i.e., in the absence of water limitations, a surface should evaporate at a rate estimated using *PET* method. We estimated *PET* using physically based Penman-Monteith method (section 2). Figure 4 compares changes in *PET* estimated in this study with *ET* changes in 20 climate models from the CMIP5. It is remarkable to see that our *PET* estimate is comparable to more complex *ET* parameterization in CMIP5 models with $R^2 \geq 0.97$ and slope $\sim$1 over oceans where there are no water limitations to evaporation. Over land, the relationship between *PET* and *ET* changes from historical ($R^2 = 0.66$) to RCP8.5 ($R^2 \sim 0$) climate projections, which could be due to an increased water limitation to evaporation [*Kumar et al*., 2013b] and carbon cycle feedback processes (discussed later). We also assessed the *PET* estimate at local scales (grid cell) and found comparable results similar to *Scheff and Frierson*, [2014] (not shown). Overall, we conclude that the FAO-based *PET* estimate is a defensible measure of atmospheric demand.

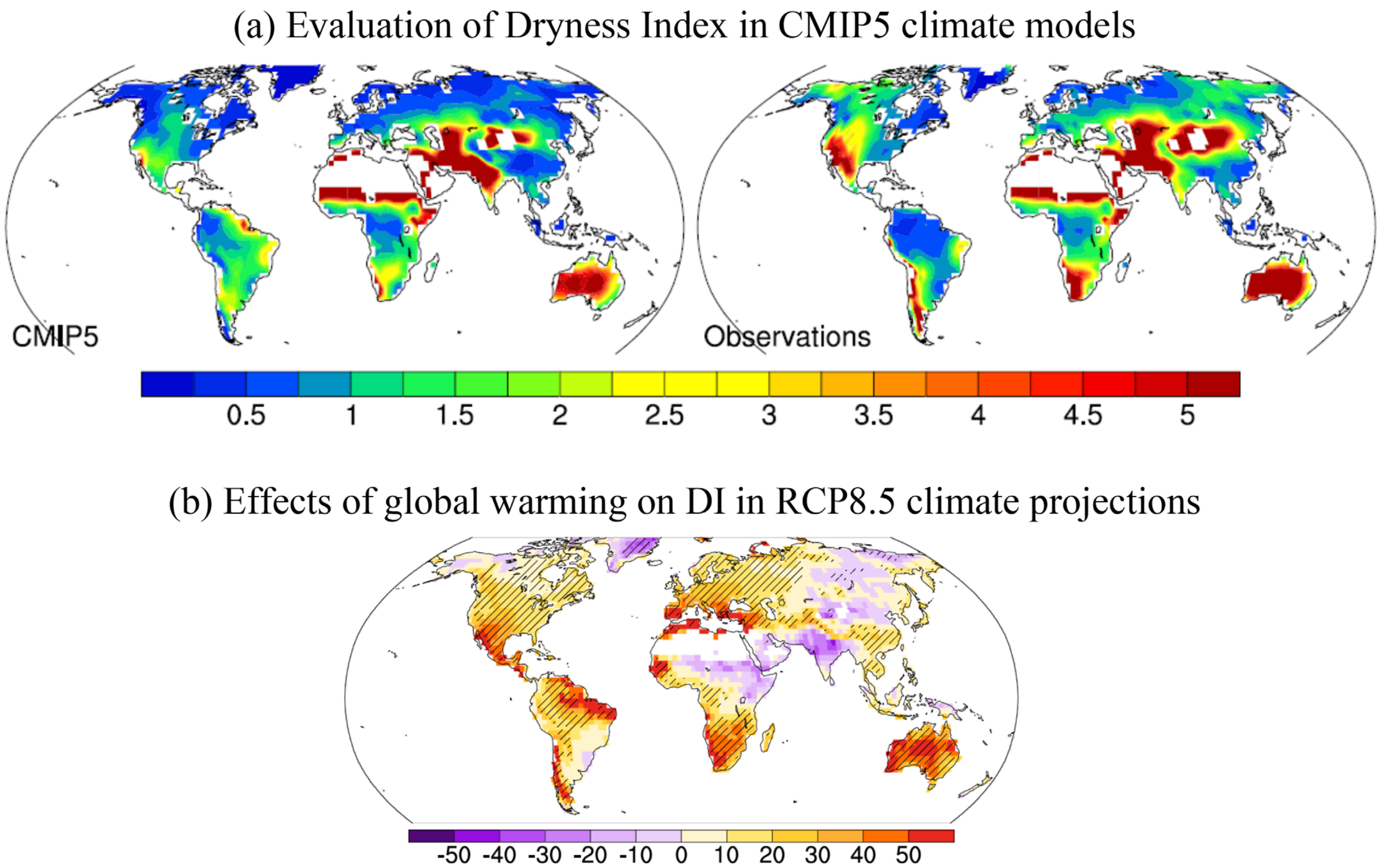

Figure 5. (a) Evaluation of the dryness index in CMIP5 models. Observations show average of three global data sets mentioned in the main text for present climate conditions (1976–2005); (b) projection of DI at the end of 21st century in RCP8.5 climate scenario, shown as the percentage difference from the historical period, i.e., (2081–2100) to (1981–200), hatching shows statistically significant differences at 5% significance level.

3.4. Evaluation of CMIP5 Models for Budyko Modeling

Figures 5a and 5b show a comparison of *DI* diagnosed from 20 CMIP5 climate models with *DI* diagnosed from observations for the last 30 years of the historical period (1976–2005). CMIP5 models adequately capture the spatial variability in observed *DI* (spatial correlation: 0.86). A small wet bias (−7%, local bias in *DI* on average) is found, which is expected given the precipitation biases in climate models, particularly wet precipitation biases in dry regions, e.g., Australia and western North America [*Flato et al*., 2013; *Sheffield et al*., 2013]. Overall, we conclude that CMIP5 models adequately describe *DI* within the observational uncertainty range, e.g., the precipitation undercatch issue in snow-dominated high-latitude regions, and the sparse observational network in less observed part of the world, e.g., South America, Africa, and Asia [*Groisman and Legates*, 1994; *Mekis and Vincent*, 2011; *Kumar et al*., 2013a]. *DI* increases in most places around the world in RCP8.5 climate projections (Figure 3c) [also see *Fu and Feng*, 2014].

Figure 6 shows an evaluation of the catchment efficiency parameter (*w*) and the effect of global warming on w. The multimodel mean estimate of *w* shows spatial variability that is consistent with the distribution of vegetation in the current climate (Figure 6a), i.e., higher *w* is found in regions with dense vegetation coverage, e.g., in the eastern United States, boreal regions of North America and Europe, the Amazon, and Congo basins, and Southeast Asia [*Li et al*., 2013; *Greve et al*., 2014]. These regions also show significant decreases in *w* during the 21st century (Figure 6b). Fewer regions, e.g., Siberia, and parts of Alaska and northwest Canada show an increase in *w*. Overall, the global average *w* decreases by 12.6% in the 21st century which indicates that several climate process, such as increased plant water use efficiency under elevated atmospheric CO_2 concentration, increased soil resistance to evaporation under drier conditions, and land use change oppose climate-driven evaporative demand on the land [*Zhang et al*., 2001; *Betts et al*., 2007; Cao et al., 2010; *Kumar et al*., 2013b].

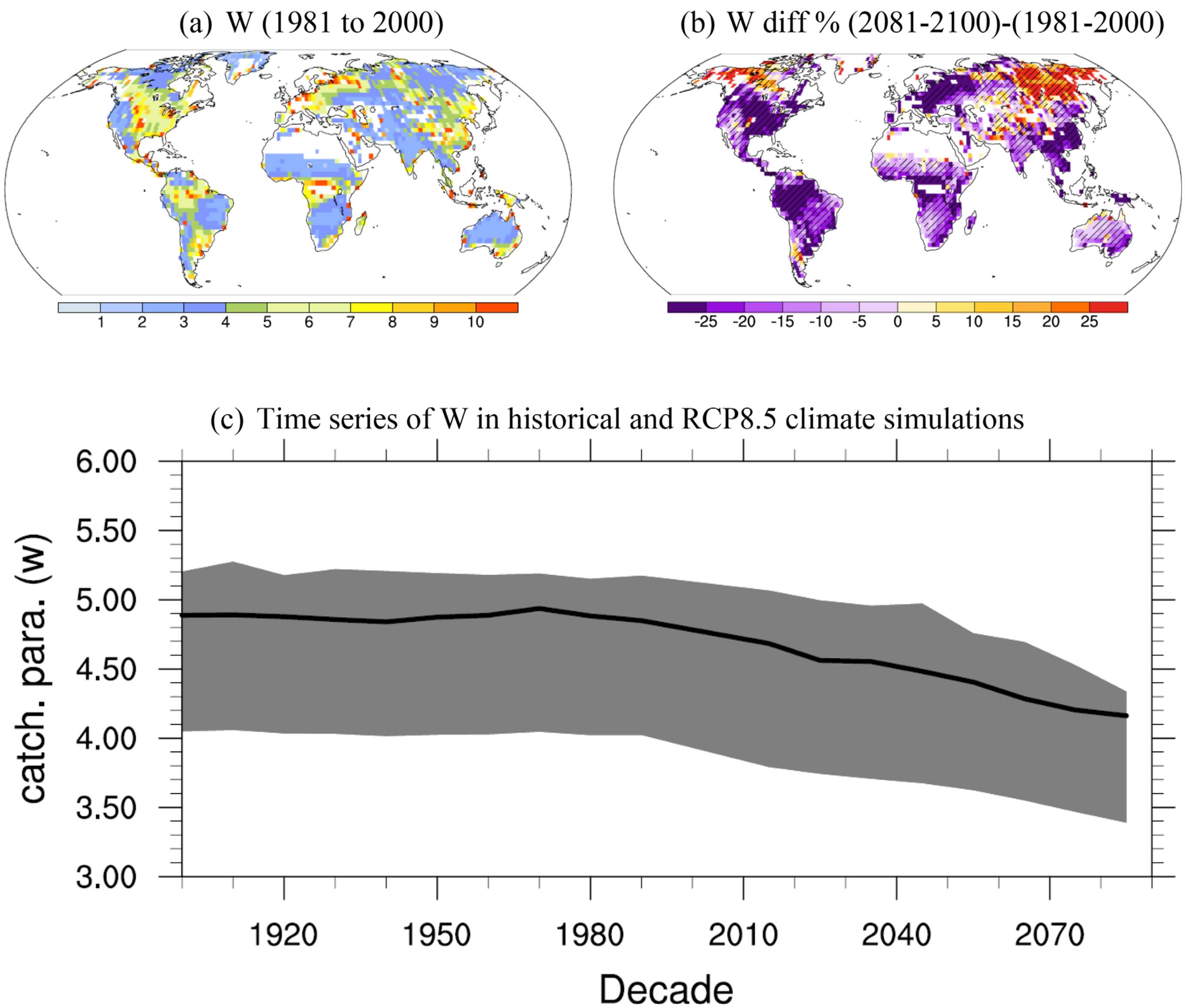

Figure 6. Evaluation of the catchment efficiency parameter (*w*) and effects of global warming: (a) estimated *w* from CMIP5 simulations in the historical period (1981–2000); (b) changes in *w* between the end of 21st century and end of 20th century where only statistically significant changes at 5% significance level are shown; (c) time series of 20 year average DI from historical and RCP8.5 climate simulations (local values averaged globally), decade on the *x* axis represents the center of the 20 year period. Please note that locations where nonlinear optimization did not converge are shown as missing values with white color.

The multimodel mean estimate of *w* from CMIP5 models is higher than typically used in the hydrology literature ($w = 1.9 + 0.72$) [*Li et al.*, 2013; *Roderick et al.*, 2014]. This is due to a higher *ET*/P ratio in climate models/land surface model than hydrologic models [*Haddeland et al.*, 2011] (also see supporting information Figures S2 and S3).

3.5. Terrestrial Hydrological Sensitivity

We study the sensitivity of hydrological changes (dRR/dDI) using the Budyko framework (equation (2a)) and compare it with the sensitivity derived from CMIP5 models

$$\left(\frac{dRR}{dDI}\right)_{CMIP5} \cong \left(\frac{\Delta RR}{\Delta DI}\right)_{CMIP5} \quad (4)$$

where ΔRR and ΔDI are computed as the difference between the last 20 year and first 20 year climatologies in historical and RCP8.5 climate simulations, respectively. We present the multimodel mean sensitivity $\left(\frac{\Delta RR}{\Delta DI}\right)$

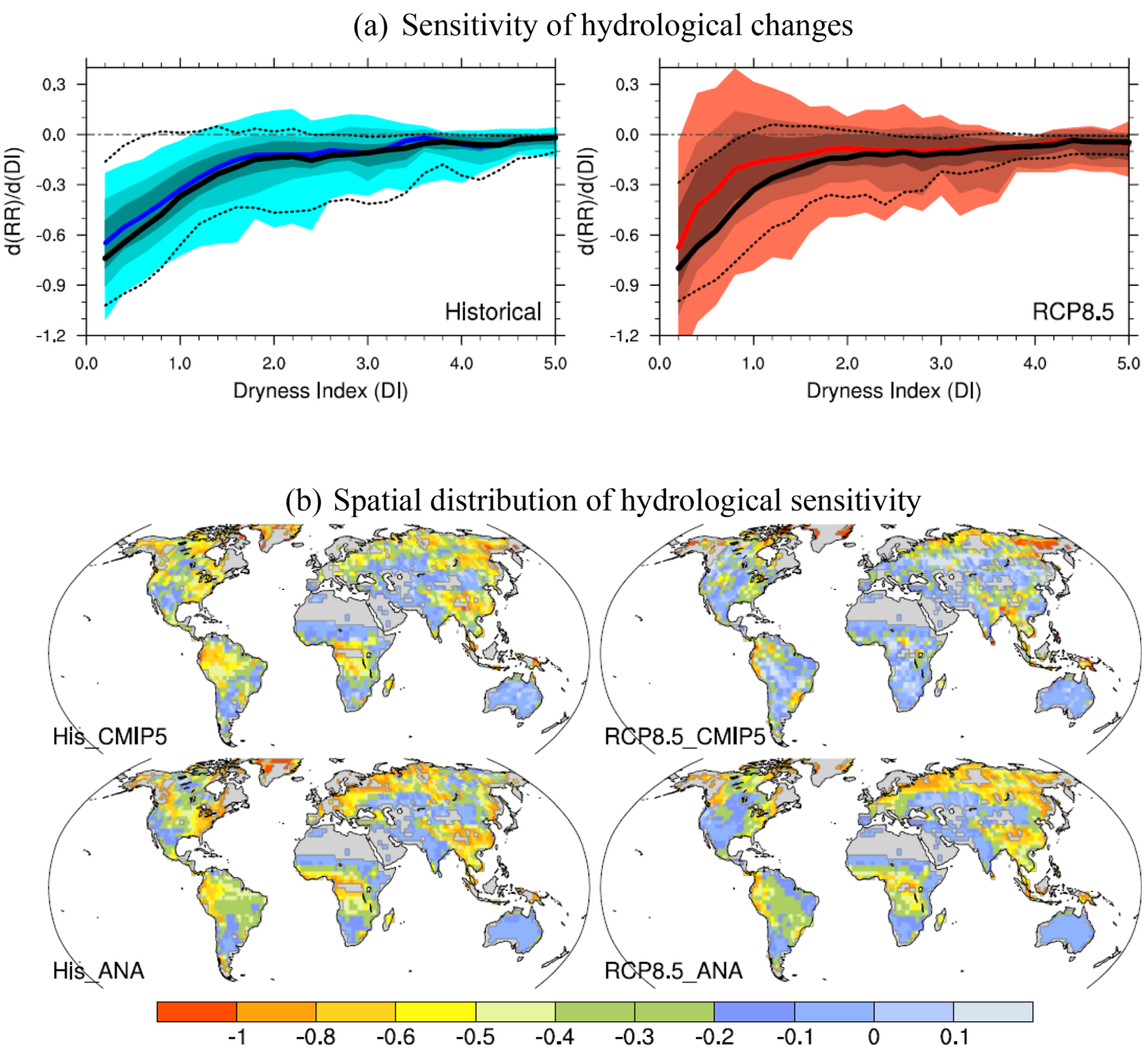

Figure 7. Effects of global warming on hydrological sensitivity: (a) sensitivity of hydrological changes in CMIP5 simulations $\left(\frac{\Delta RR}{\Delta DI}\right)$ and from the Budyko framework $\left(\frac{dRR}{dDI}\right)$ (ANA, equation (2a), see text). Colored lines and shading show CMIP5 results, and analytical expression results are shown by black thick line (spatial median) and dashed lines (95% spatial variability range). Colored thick lines show the spatial median of CMIP5 results, and shading shows 50%, 75%, and 95% spatial ranges in the order of darker to lighter shading, (b) global map of the hydrological sensitivity in CMIP5 simulations and analytical expression. Locations where nonlinear optimization for catchment efficiency parameter did not converge are shown as missing values in gray shading.

from the CMIP5 models and mean of a distribution of 500 analytically derived $\left(\frac{dRR}{dDI}\right)$ using CMIP5 estimates of *w*, *DI*, and *dw/dDI*. This distribution is obtained by a normally distributed random sample of *w* and *dw/dDI* values covering their 95% uncertainty range and uniformly sampled *DI*; these values correspond to the mid-21st and 20th century values in RCP8.5 and historical simulations, respectively.

Figure 7 shows the sensitivity of hydrological changes in historical and future climate simulations. The Budyko framework describes regional and local variations in hydrological sensitivity reasonably well, particularly in the historical period. A greater hydrological sensitivity is found in generally wet regions, e.g., eastern North America, the U.S. plains, and Canada, high-latitude regions, the Amazon and Congo basins, and

Table 2. Sensitivity of Terrestrial Hydrological Changes [dRR/dDI][a]

Climate Simulations	Energy Limited (Wet)	Water Limited (Dry)	Ratio (Wet/Dry)
Historical, CMIP5	−0.53 (±0.23)	−0.18 (±0.18)	2.9
RCP8.5, CMIP5	−0.33 (±0.38)	−0.12 (±0.19)	2.8
Historical, ANA (equation (2a))	−0.57 (±0.26)	−0.20 (±0.16)	2.8
RCP8.5, ANA (equation (2a))	−0.53 (±0.24)	−0.16 (±0.15)	3.3

[a]Numbers in parenthesis show ± 1 standard deviation of spatial variability.

south-east Asia (Figure 7b, and Table 2). Dry regions such as the southwestern United States, Sahel, central Asia, and Australia show a lower hydrological sensitivity.

The hydrological sensitivity is generally reduced in future climate (Table 2). Direct calculations from CMIP5 models $\left(\frac{\Delta RR}{\Delta DI}\right)$ indicate a greater reduction in hydrological sensitivity in wet regions than estimated using the Budyko framework $\left(\frac{dRR}{dDI}\right)$ (Figures 7a and 7b, right column). The analytical solution also suggests a reduction in sensitivity in several regions, e.g., North and South America. The future projections of hydrological sensitivity based on the Budyko framework show a better correspondence with their historical sensitivity (spatial correlation between left and right columns of bottom row in Figure 7b: 0.79) than directly calculated from CMIP5 data (spatial correlation: 0.51, same as before for top row in Figure 7b). Overall, both CMIP5 simulations and the analytical expression suggest heterogeneity in sensitivity of hydrological changes where wet regions experience 3 times higher hydrological sensitivity than dry regions (Table 2).

The estimated sensitivity under the Budyko framework is strongly controlled by the second term in equation (2a), i.e., whether the sensitivity of the catchment efficiency parameter is considered or not. If it is not considered ($dw/dDI = 0$) then a biased estimate of the hydrological sensitivity results, particularly in the wet

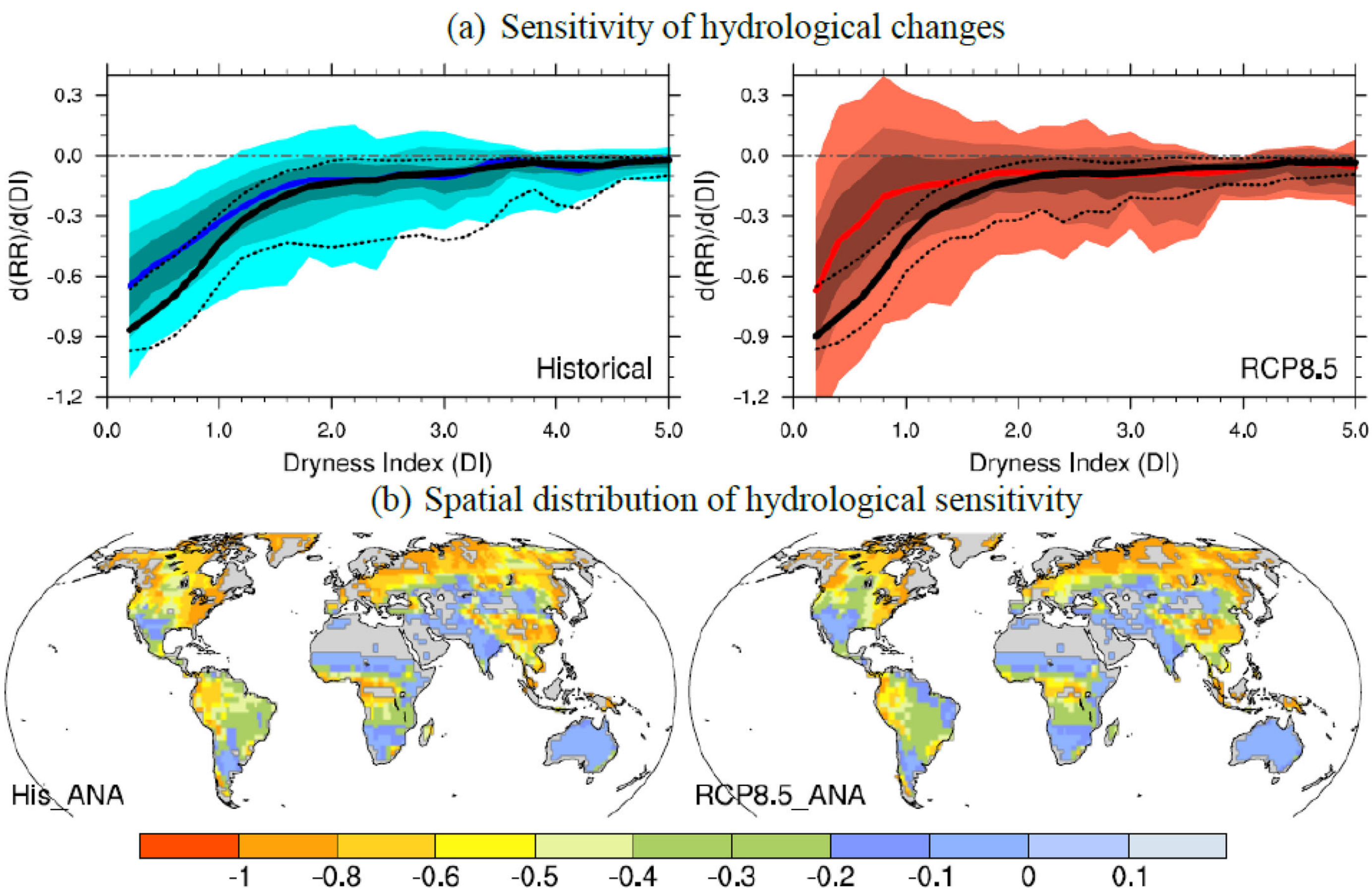

Figure 8. Same as Figure 7 but using only first term from equation (2a), i.e., $dw/dDI = 0$.

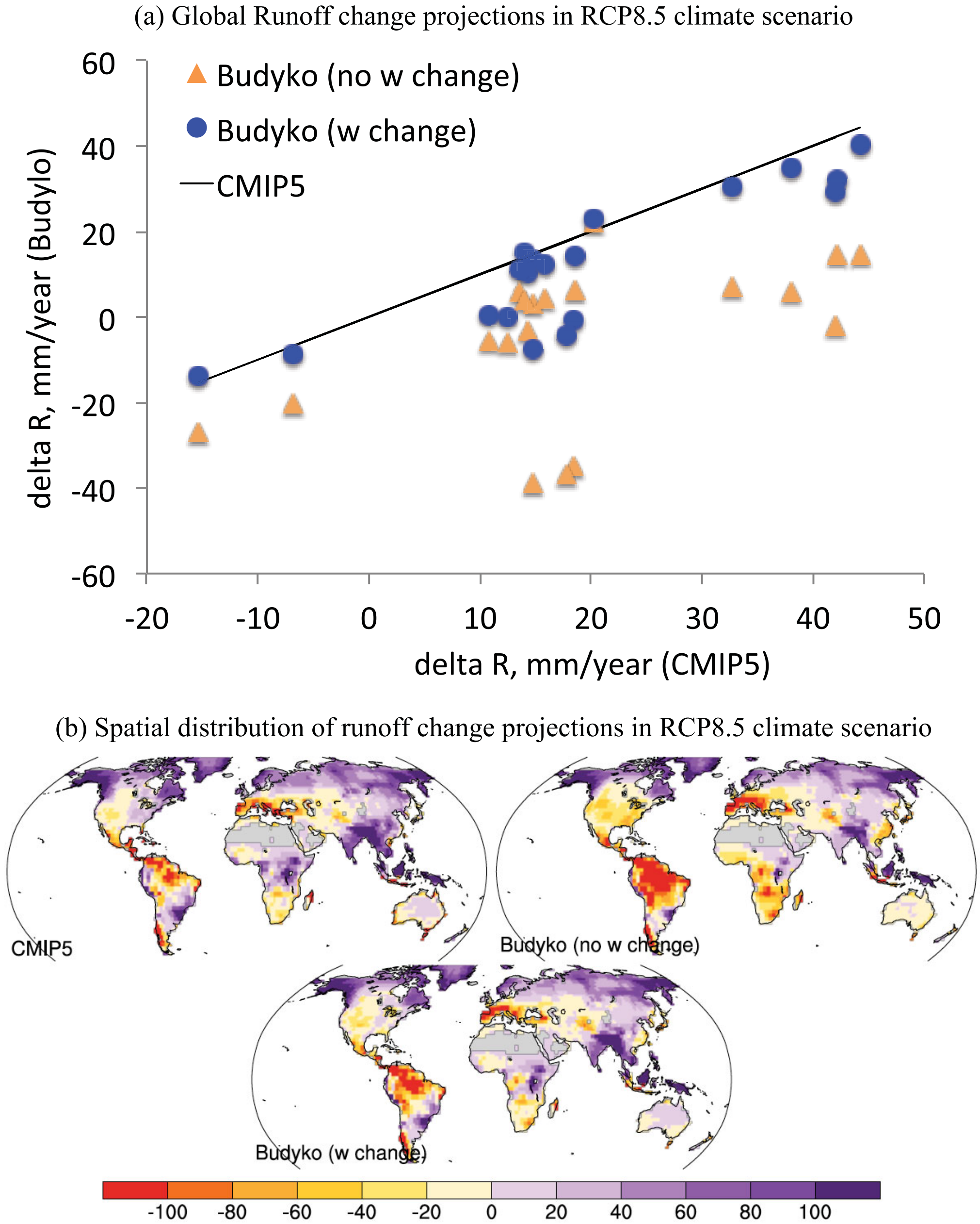

Figure 9. (a) Global runoff change projections in 19 CMIP5 climate models, and using the Budyko framework with and without change in *w*. Runoff change projections for the RCP8.5 climate scenario are shown as the difference between last and first 20 years, i.e., (2081–2100) to (2006–2025). (b) Spatial distribution of multimodel mean runoff change projections.

regions (Figure 8). Results shown in Figure 7 are minimally sensitive if we use *w* and *DI* from the base period, i.e., first 20 year of historical or RCP8.5 climate simulation (not shown); thus, providing a predictive power in Budyko framework.

3.6. Effects of "w" Parameter Change on Runoff Projections

Figure 9 and Table 3 show effects of the change in the catchment efficiency parameter on global runoff change projections. Runoff change projections using the Budyko framework are obtained by employing the change in *DI* and precipitation from CMIP5 models; in one case, change in the catchment efficiency parameter is also incorporated (with *w* change), and in other case, values from the base period is used (no *w* change). Least square estimates of *w* from individual climate model are employed here. It is evident that reduction in the catchment efficiency parameter significantly reduces dry biases. In RCP8.5, projections

10.1002/2016WR018607

Table 3. Global Runoff Change Projections in CMIP5 Models and Using Budyko Framework With and Without Changes in the Catchment Efficiency Parameter[a]

	Historical ((1981 to 2000) - (1881 to 1900))		RCP8.5 ((2076 to 2095) - (2006 to 2025))	
	Runoff Change (mm/yr)	Spatial Correlation	Runoff Change (mm/yr)	Spatial Correlation
CMIP5	−1.4	1	19.1	1
Budyko (no w change)	−5.0	0.91	−4.5	0.87
Budyko (w change)	−3.2	0.94	12.2	0.94

[a]Multimodel mean results are shown here.

biases are reduced from −4.5 mm/yr (no *w* change) to 12.2 mm/yr (with *w* change), which is closer to CMIP5 projections of 19.1 mm/yr (Table 3). For example, a strong drying in most places in North America is significantly reduced after incorporating the change in the catchment efficiency parameter (Figure 9b). Similar improvements in runoff change projections are also found in South America, Africa, Mediterranean, and Australia. The spatial correlation between Budyko-based runoff change projections and CMIP5 remains similar with or without change in catchment efficiency parameter (Table 3).

One caveat in the analysis presented in Figure 9 and Table 3 is that we assume that the change in the catchment efficiency parameter is known beforehand. The main purpose of this analysis was to demonstrate the effects of the decrease in the catchment efficiency parameter on runoff projections.

4. Discussion and Conclusions

There is a relatively robust understanding of changes in the atmospheric branch of hydrological cycle where wet regions are expected to experience greater hydrological changes [*Chou and Neelin*, 2004; *Held and Soden*, 2006; *Seager et al*., 2010]. The terrestrial branch remains less well understood, with substantial observational uncertainty and limited evidence of detectable change over the historical period [*Greve et al*., 2014]. An additional factor may be that the terrestrial branch of the hydrological cycle may contribute to the spatial heterogeneity in hydrological changes. The terrestrial hydrological sensitivity and detectability of streamflow changes are found to be greater in the regions where the hydrological cycle is energy limited. An analogy using a simple Bucket Hydrology model [*Manabe*, 1969] can be drawn here—in wet regions, the bucket is relatively full, hence a higher fraction of precipitation variability and changes result in runoff changes; whereas in dry regions, the bucket is empty, i.e., a large buffer is available to dampen precipitation variability and changes leading to smaller runoff changes [*Koster and Suarez*, 1999; *Sankarasubramanian and Vogel*, 2002; *Zhang et al*., 2008].

The terrestrial hydrological sensitivity (dRR/dDI) concept outlined in this study differs from the concept of precipitation elasticity of runoff in the following ways: (1) here we assess absolute changes in *RR* compared to proportional changes in runoff in the elasticity concept [*Schake*, 1990; *Sankarasubramanian et al*., 2001; *Vano et al*., 2012], and (2) by assessing changes with respect to *DI*, we implicitly incorporate changes in potential evaporation that increase at a much faster rate (5–6% $°C^{-1}$ of warming) than precipitation changes (1–2% $°C^{-1}$ of warming) [*Held and Soden*, 2006; *Scheff and Frierson*, 2014; *Roderick et al*., 2015; *Fu and Feng*, 2014]. The precipitation elasticity concept does not incorporate changes in potential evaporation, which negatively impacts precipitation elasticity. Importantly, this new concept helps us to understand additional (terrestrial) sources of the higher detectability of hydrological changes in energy limited regions compared to water-limited regions, which is supported by observational evidence and climate model simulation results (Figures 1 and 2).

A generally decreased hydrological sensitivity in the 21st century than the 20th century could be due to several factors including (1) increased dryness, (2) a decrease in *w* due to increased plants' water use efficiency and land use changes, and (3) a negative sensitivity of *w* to the increase in *DI* (supporting information Figure S6). To the authors' knowledge, this is the first study to quantify sensitivity of the catchment efficiency parameter (dW/dDI) at global scales, which has previously been discussed only qualitatively [e.g., *Roderick and Farquhar*, 2011; *Roderick et al*., 2014]. Incorporation of $\frac{dW}{dDI}$ within the Budyko framework reduces the magnitude of hydrological sensitivity, with the catchment efficiency parameter acting in a self-regulating manner that opposes climate-driven changes. It also reduces dry biases in runoff change projections by 88% in the 21st century. *Zhang et al*. [2015b] found resilience in crops to drought stresses using long-term observations in semiarid regions of Northern China.

We employed a physically based estimate of potential evaporation using Penman-Monteith method similar to other studies, e.g., *Sheffield et al*. [2012], *Cook et al*. [2014], and *Fu and Feng* [2014]. *Shuttleworth* [2012] strongly recommends the Penman-Monteith method as the preferred method to estimate *PET*. *Roderick et al*. [2015] found that global land evaporation does not follow increasing potential evaporation under global warming scenario hence they suggested using net radiation instead of potential evaporation for computing *DI* [e.g., *Roderick et al*., 2014]. Net radiation increases globally but with a much smaller magnitude (39 mm/yr/century) than potential evaporation (230 mm/yr/century) [*Roderick et al*., 2015; also see *Greve and Seneviratne*, 2015]. One major implication of using net radiation is that it results in a different interpretation of the changes in *w*, such that the catchment efficiency parameter slightly increases or remains the same under elevated CO_2 concentration, and global warming conditions (supporting information Figure S7). Overall, a similar runoff change projection can be obtained using two different methods: (1) using Penman-Monteith-based *PET* and a decrease in *w* (this study), and (2) using Rn as *PET*, and no change in *w* [e.g., *Roderick et al*., 2014].

There are significant differences in using Rn only as *PET* than Penman-Monteith method. Using Rn as measure of atmospheric demand ignores the aerodynamic component that can account for approximately 30% of energy (Rn)-driven demand, also known as the Priestley-Taylor method [*Chow et al*., 1988]. *Greve and Seneviratne* [2015] found that global land areas showing significant changes in *DI* almost doubles when using Priestely-Taylor method for *PET* compared to Rn only as *PET*. Further, we present a physically plausible explanation for decrease in w, e.g., increased water use efficiency under elevated CO_2 concentration, increased soil resistance under drier conditions, and land use change.

The Budyko framework provides an alternative approach (other than CMIP5) for hydrological change assessment; independent estimates of *DI* and *w* can potentially be used to study hydrological changes at watershed scales [e.g., *Jiang et al*., 2015]. Parsimony in the Budyko framework enables us to study parameter sensitivity in more details than global climate models where sensitivity of several parameters, e.g., drought stress and phenology scheme are not discussed in comparable details [*Basu et al*., 2010; *Dirmeyer et al*., 2013; *Dahlin et al*., 2015]. We also found uncertainty in future projections of hydrological sensitivity using the Budyko framework. Changes in the catchment efficiency parameter are an important source of uncertainty in future water projections based on the Budyko framework.

Acknowledgments

S.K. and F.Z. were supported by NSERC Canadian Sea Ice and snow Evaluation (CanSISE) Network. The first author thanks Markus Schnorbus and Faron Anslow (both from PCIC) for providing hydrology data for watersheds in British Columbia. The first author also thanks Justin Sheffield (Princeton University) for providing Princeton Hydrology data. We acknowledge the World Climate Research Programme's Working Group on Coupled Modelling, which is responsible for CMIP, and we thank the climate modeling groups (listed in supporting information Table S1) for producing and making available their model output. CMIP5 climate model data were obtained from following website: https://pcmdi9.llnl.gov/projects/esgf-llnl/. Streamflow data were obtained from United States Geological Survey (http://waterdata.usgs.gov/nwis/uv/?referred_module=sw) and Environment Canada HYDAT database (https://ec.gc.ca/rhc-wsc/default.asp?lang=En&n=9018B5EC-1) for western United States and Western Canada, respectively. High-resolution PRISM climate data were provided by PRISM Climate Group, Oregon State University, http://prism.oregonstate.edu, created 4 February 2004. We also thank Michael L. Roderick and one anonymous reviewer for their constructive comments on earlier versions of this manuscript.

References

Alkama, R., L. Marchand, A. Ribes, and B. Decharme (2013), Detection of global runoff changes: Results from observations and CMIP5 experiments, *Hydrol. Earth Syst. Sci.*, *17*(7), 2967–2979, doi:10.5194/hess-17-2967-2013.

Allan, R. P. (2014), Climate change: Dichotomy of drought and deluge, *Nat. Geosci.*, *7*(10), 700–701, doi:10.1038/ngeo2243.

Allen, R. G., M. Smith, L. S. Pereira, and A. Perrier (1994), An update for the calculation of reference evapotranspiration, *ICID Bull.*, *43*, 35–92.

Basu, N. B., P. S. C. Rao, H. E. Winzeler, S. Kumar, P. Owens, and V. Merwade (2010), Parsimonious modeling of hydrologic responses in engineered watersheds: Structural heterogeneity versus functional homogeneity, *Water Resour. Res.*, *46*, W04501, doi:10.1029/2009WR007803.

Berghuijs, W. R., R. A. Woods, and M. Hrachowitz (2014), A precipitation shift from snow towards rain leads to a decrease in streamflow, *Nat. Clim. Change*, *4*(7), 583–586, doi:10.1038/nclimate2246.

Betts, R. A., et al. (2007), Projected increase in continental runoff due to plant responses to increasing carbon dioxide, *Nature*, *448*(7157), 1037–1041, doi:10.1038/nature06045.

Budyko, M. I. (1958), *The Heat Balance of the Earth's Surface*, US Dep. of Commer., Washington, D. C.

Cao, L., G. Bala, K. Caldeira, R. Nemani, and G. Ban-Weiss (2010), Importance of carbon dioxide physiological forcing to future climate change, *Proc. Natl. Acad. Sci. U. S. A.*, *107*(21), 9513–9518, doi:10.1073/pnas.0913000107.

Chadwick, R., I. Boutle, and G. Martin (2012), Spatial patterns of precipitation change in CMIP5: Why the rich do not get richer in the tropics, *J. Clim.*, *26*(11), 3803–3822, doi:10.1175/JCLI-D-12-00543.1.

Chen, J., F. P. Brissette, D. Chaumont, and M. Braun (2013), Performance and uncertainty evaluation of empirical downscaling methods in quantifying the climate change impacts on hydrology over two North American river basins, *J. Hydrol.*, *479*, 200–214, doi:10.1016/j.jhydrol.2012.11.062.

Chou, C., and J. D. Neelin (2004), Mechanisms of global warming impacts on regional tropical precipitation*, *J. Clim.*, *17*(13), 2688–2701, doi:10.1175/1520-0442(2004)017<2688:MOGWIO>2.0.CO;2.

Chow, V., et al. (1988), *Applied Hydrology*, pp. 80–93, McGraw-Hill, N. Y.

Dahlin, K. M., R. A. Fisher, and P. J. Lawrence (2015), Environmental drivers of drought deciduous phenology in the community land model, *Biogeosci. Discuss.*, *12*, 5803–5839.

Dai, A., T. Qian, K. E. Trenberth, and J. D. Milliman (2009), Changes in continental freshwater discharge from 1948 to 2004, *J. Clim.*, *22*(10), 2773–2792, doi:10.1175/2008JCLI2592.1.

Daly, C., M. Halbleib, J. I. Smith, W. P. Gibson, M. K. Doggett, G. H. Taylor, J. Curtis, and P. P. Pasteris (2008), Physiographically sensitive mapping of climatological temperature and precipitation across the conterminous United States, *Int. J. Climatol.*, *28*(15), 2031–2064, doi:10.1002/joc.1688.

Deser, C., R. Knutti, S. Solomon, and A. S. Phillips (2012), Communication of the role of natural variability in future North American climate, *Nat. Clim. Change*, *2*(11), 775–779, doi:10.1038/nclimate1562.

Dirmeyer, P. A., S. Kumar, M. J. Fennessy, E. L. Altshuler, T. DelSole, Z. Guo, B. A. Cash, and D. Straus (2013), Model estimates of land-driven predictability in a changing climate from CCSM4, *J. Clim.*, *26*(21), 8495–8512, doi:10.1175/JCLI-D-13-00029.1.

Flato, G., et al. (2013), Evaluation of climate models, in *Climate Change 2013: The Physical Science Basis. Contribution of Working Group I to the Fifth Assessment Report of the Intergovernmental Panel on Climate Change*, edited by T. F. Stocker et al., pp. 741–866, Cambridge Univ. Press, Cambridge, U. K.

Fu, Q., and S. Feng (2014), Responses of terrestrial aridity to global warming, *J. Geophys. Res. Atmos.*, *119*, 7863–7875, doi:10.1002/2014JD021608.

Greve, P., and S. I. Seneviratne (2015), Assessment of future changes in water availability and aridity, *Geophys. Res. Lett.*, *42*, 5493–5499, doi:10.1002/2015GL064127.

Greve, P., B. Orlowsky, B. Mueller, J. Sheffield, M. Reichstein, and S. I. Seneviratne (2014), Global assessment of trends in wetting and drying over land, *Nat. Geosci.*, *7*(10), 716–721, doi:10.1038/ngeo2247.

Greve, P., L. Gudmundsson, B. Orlowsky, and S. I. Seneviratne (2015), Introducing a probabilistic Budyko framework, *Geophys. Res. Lett.*, *42*, 2261–2269, doi:10.1002/2015GL063449.

Groisman, P. Y., and D. R. Legates (1994), The accuracy of United States precipitation data, *Bull. Am. Meteorol. Soc.*, *75*(2), 215–227, doi:10.1175/1520-0477(1994)075 < 0215:TAOUSP>2.0.CO;2.

Haddeland, I., et al. (2011), Multimodel estimate of the global terrestrial water balance: Setup and first results, *J. Hydrometeorol.*, *12*(5), 869–884, doi:10.1175/2011JHM1324.1.

Hagemann, S., C. Chen, J. O. Haerter, J. Heinke, D. Gerten, and C. Piani (2011), Impact of a statistical bias correction on the projected hydrological changes obtained from three GCMs and two hydrology models, *J. Hydrometeorol.*, *12*(4), 556–578, doi:10.1175/2011JHM1336.1.

Harris, I., P. D. Jones, T. J. Osborn, and D. H. Lister (2014), Updated high-resolution grids of monthly climatic observations—The CRU TS3.10 Dataset, *Int. J. Climatol.*, *34*(3), 623–642, doi:10.1002/joc.3711.

Held, I. M., and B. J. Soden (2006), Robust responses of the hydrological cycle to global warming, *J. Clim.*, *19*(21), 5686–5699, doi:10.1175/JCLI3990.1.

Herring, S. C., M. P. Hoerling, T. C. Peterson, and P. A. Stott (Eds.) (2014), Explaining extreme events of 2013 from a climate perspective, *Bull. Am. Meteorol. Soc.*, *95*(9), supplement, 1–96.

Jiang, C., L. Xiong, D. Wang, P. Liu, S. Guo, and C.-Y. Xu (2015), Separating the impacts of climate change and human activities on runoff using the Budyko-type equations with time-varying parameters, *J. Hydrol.*, *522*, 326–338.

Jimenez Cisneros, B. E., T. Oki, N. W. Arnell, G. Benito, J. G. Cogley, P. Doll, T. Jiang, and S. S. Mwakalila (2014), Freshwater resources, in *Climate Change 2014: Impacts, Adaptation and Vulnerability. Part A: Global and Sectoral Aspects. Contribution of Working Group II to the Fifth Assessment Report of the Intergovernmental Panel on Climate Change*, edited by C. B. Field et al., pp. 229–269, Cambridge Univ. Press, Cambridge.

Jones, G. S., P. A. Stott, and N. Christidis (2013), Attribution of observed historical near-surface temperature variations to anthropogenic and natural causes using CMIP5 simulations, *J. Geophys. Res. Atmos.*, *118*, 4001–4024, doi:10.1002/jgrd.50239.

Koster, R. (2014), ''Efficiency Space'': A framework for evaluating joint evaporation and runoff behavior, *Bull. Am. Meteorol. Soc.*, *96*(3), 393–396, doi:10.1175/BAMS-D-14-00056.1.

Koster, R. D., and M. J. Suarez (1999), A simple framework for examining the interannual variability of land surface moisture fluxes, *J. Clim.*, *12*(7), 1911–1917, doi:10.1175/1520-0442(1999)012 < 1911:ASFFET>2.0.CO;2.

Kumar, S., V. Merwade, J. Kam, and K. Thurner (2009), Streamflow trends in Indiana: Effects of long term persistence, precipitation and subsurface drains, *J. Hydrol.*, *374*(1–2), 171–183, doi:10.1016/j.jhydrol.2009.06.012.

Kumar, S., V. Merwade, J. L. Kinter III, and D. Niyogi (2013a), Evaluation of temperature and precipitation trends and long-term persistence in CMIP5 twentieth-century climate simulations, *J. Clim.*, *26*, 4168–4185.

Kumar, S., P. A. Dirmeyer, V. Merwade, T. DelSole, J. M. Adams, and D. Niyogi (2013b), Land use/cover change impacts in CMIP5 climate simulations: A new methodology and 21st century challenges, *J. Geophys. Res. Atmos.*, *118*, 6337–6353, doi:10.1002/jgrd.50463.

Kumar, S., R. P. Allan, F. Zwiers, D. M. Lawrence, and P. A. Dirmeyer (2015), Revisiting trends in wetness and dryness in the presence of internal climate variability and water limitations over land, *Geophys. Res. Lett.*, *42*, 10,867–10,875, doi:10.1002/2015GL066858.

Lawrence, D. M., et al. (2011), Parameterization improvements and functional and structural advances in version 4 of the Community Land Model, *J. Adv. Model. Earth Syst.*, *3*, M03001, doi:10.1029/2011MS000045.

Li, D., M. Pan, Z. Cong, L. Zhang, and E. Wood (2013), Vegetation control on water and energy balance within the Budyko framework, *Water Resour. Res.*, *49*, 969–976, doi:10.1002/wrcr.20107.

Manabe, S. (1969), Climate and the ocean circulation1, *Mon. Weather Rev.*, *97*(11), 739–774, doi:10.1175/1520-0493(1969)097 < 0739:CATOC>2.3.CO;2.

Mekis, É., and L. A. Vincent (2011), An overview of the second generation adjusted daily precipitation dataset for trend analysis in Canada, *Atmos. Ocean*, *49*(2), 163–177, doi:10.1080/07055900.2011.583910.

Milly, P. C. D. (1994), Climate, soil water storage, and the average annual water balance, *Water Resour. Res.*, *30*(7), 2143–2156, doi:10.1029/94WR00586.

Milly, P. C. D., K. A. Dunne, and A. V. Vecchia (2005), Global pattern of trends in streamflow and water availability in a changing climate, *Nature*, *438*(7066), 347–350, doi:10.1038/nature04312.

Oleson, K. W., et al. (2010), Technical description of version 4.0 of the Community Land Model (CLM), *NCAR Tech. Note NCAR/TN-478+STR*, National Center for Atmospheric Research, Boulder, Colo.

Roderick, M. L., and G. D. Farquhar (2011), A simple framework for relating variations in runoff to variations in climatic conditions and catchment properties, *Water Resour. Res.*, *47*, W00G07, doi:10.1029/2010WR009826.

Roderick, M. L., F. Sun, W. H. Lim, and G. D. Farquhar (2014), A general framework for understanding the response of the water cycle to global warming over land and ocean, *Hydrol. Earth Syst. Sci.*, *18*(5), 1575–1589, doi:10.5194/hess-18-1575-2014.

Roderick, M. L., P. Greve, and G. D. Farquhar (2015), On the assessment of aridity with changes in atmospheric CO_2, *Water Resour. Res.*, *51*, 5450–5463, doi:10.1002/2015WR017031.

Sagarika, S., A. Kalra, and S. Ahmad (2014), Evaluating the effect of persistence on long-term trends and analyzing step changes in streamflows of the continental United States, *J. Hydrol.*, *517*, 36–53, doi:10.1016/j.jhydrol.2014.05.002.

Sankarasubramanian, A., and R. M. Vogel (2002), Annual hydroclimatology of the United States, *Water Resour. Res.*, *38*(6), doi:10.1029/2001WR000619.

Sankarasubramanian, A., R. M. Vogel, and J. F. Limbrunner (2001), Climate elasticity of streamflow in the United States, *Water Resour. Res.*, *37*(6), 1771–1781.

Santer, B. D., et al. (2007), Identification of human-induced changes in atmospheric moisture content, *Proc. Natl. Acad. Sci. U. S. A.*, *104*(39), 15,248–15,253, doi:10.1073/pnas.0702872104.

Seager, R., N. Naik, and G. A. Vecchi (2010), Thermodynamic and dynamic mechanisms for large-scale changes in the hydrological cycle in response to global warming*, *J. Clim.*, *23*(17), 4651–4668, doi:10.1175/2010JCLI3655.1.

Seager, R., M. Hoerling, S. Schubert, H. Wang, B. Lyon, A. Kumar, J. Nakamura, and N. Henderson, (2015), Causes of the 2011–14 California drought, *J. Clim.*, *28*, 6997–7024, doi:10.1175/JCLI-D-14-00860.1.

Scheff, J., and D. M. W. Frierson (2014), Scaling potential evapotranspiration with greenhouse warming, *J. Clim.*, *27*, 1539–1558, doi:10.1175/JCLI-D-13-00233.1.

Schaake, J. C. (1990), From climate to flow, in *Climate Change and U.S. Water Resources*, edited by P. E. Waggoner, pp. 177–206, John Wiley.

Sheffield, J., E. F. Wood, and M. L. Roderick (2012), Little change in global drought over the past 60 years, *Nature*, *491*(7424), 435–438, doi:10.1038/nature11575.

Sheffield, J., et al. (2013), North American climate in CMIP5 experiments. Part I: Evaluation of historical simulations of continental and regional climatology, *J. Clim.*, *26*, 9209–9245.

Shuttleworth, W. J. (2012), Daily estimates of evaporation, in *Terrestrial Hydrometeorology*, pp. 334–358, John Wiley, Chichester, U. K., doi:10.1002/9781119951933.ch23.

Stahl, K., H. Hisdal, J. Hannaford, L. M. Tallaksen, H. A. J. van Lanen, E. Sauquet, S. Demuth, M. Fendekova, and J. Jódar (2010), Streamflow trends in Europe: Evidence from a dataset of near-natural catchments, *Hydrol. Earth Syst. Sci.*, *14*(12), 2367–2382, doi:10.5194/hess-14-2367-2010.

Taylor, K. E., R. J. Stouffer, and G. A. Meehl (2011), An overview of CMIP5 and the experiment design, *Bull. Am. Meteorol. Soc.*, *93*(4), 485–498, doi:10.1175/BAMS-D-11-00094.1.

Trenberth, K. E., A. Dai, G. van der Schrier, P. D. Jones, J. Barichivich, K. R. Briffa, and J. Sheffield (2014), Global warming and changes in drought, *Nat. Clim. Change*, *4*(1), 17–22, doi:10.1038/nclimate2067.

Vano, J. A., T. Das, and D. Lettenmaier (2012), Hydrologic sensitivity of Colorado River runoff to changes in precipitation and temperature, *J. Hydrometeorol.*, *13*, 932–949.

Vano, J. A., et al. (2013), Understanding uncertainties in future Colorado River streamflow, *Bull. Am. Meteorol. Soc.*, *95*(1), 59–78, doi:10.1175/BAMS-D-12-00228.1.

Wan, H., X. Zhang, F. Zwiers, and S.-K. Min (2014), Attributing northern high-latitude precipitation change over the period 1966–2005 to human influence, *Clim. Dyn.*, *45*, 1713–1726, doi:10.1007/s00382-014-2423-y.

Zhang, D., Z. Cong, G. Ni, D. Yang, and S. Hu (2015), Effects of snow ratio on annual runoff within the Budyko framework, *Hydrol. Earth Syst. Sci.*, *19*(4), 1977–1992, doi:10.5194/hess-19-1977-2015.

Zhang, J., et al. (2015b), Responses of crop water use efficiency to climate change and agronomic measures in the semiarid area of Northern China, *PLoS ONE*, *10*(9), e0137409, doi:10.1371/journal.pone.0137409.

Zhang, L., W. R. Dawes, and G. R. Walker (2001), Response of mean annual evapotranspiration to vegetation changes at catchment scale, *Water Resour. Res.*, *37*(3), 701–708, doi:10.1029/2000WR900325.

Zhang, L., K. Hickel, W. R. Dawes, F. H. S. Chiew, A. W. Western, and P. R. Briggs (2004), A rational function approach for estimating mean annual evapotranspiration, *Water Resour. Res.*, *40*, W02502, doi:10.1029/2003WR002710.

Zhang, L., N. Potter, K. Hickel, Y. Zhang, and Q. Shao (2008), Water balance modeling over variable time scales based on the Budyko framework—Model development and testing, *J. Hydrol.*, *360*(1–4), 117–131, doi:10.1016/j.jhydrol.2008.07.021.

Zhang, X., F. W. Zwiers, G. C. Hegerl, F. H. Lambert, N. P. Gillett, S. Solomon, P. A. Stott, and T. Nozawa (2007), Detection of human influence on twentieth-century precipitation trends, *Nature*, *448*(7152), 461–465, doi:10.1038/nature06025.